J Therm Anal Calorim (2016) 125:205–214
DOI 10.1007/s10973-016-5402-1

Thermal properties of ZnO and bimetallic Ag–Cu alloy reinforced poly(lactic acid) nanocomposite films

Jasim Ahmed[1] · Yasir Ali Arfat[1] · Edgar Castro-Aguirre[2] · Rafael Auras[2]

Received: 29 August 2015 / Accepted: 11 March 2016 / Published online: 24 March 2016
© Akadémiai Kiadó, Budapest, Hungary 2016

Abstract Poly(lactic acid) (PLA)-based nanocomposite films were prepared by incorporating zinc oxide (ZnO) (<50 and <100 nm) and bimetallic Ag–Cu alloy (<100 nm) nanoparticles (NP), and polyethylene glycol as a plasticizer via a solvent casting method. Thermal properties of the nanocomposites films were investigated using differential scanning calorimeter and thermogravimetric analyzer. The addition of 20 % PEG to the neat-PLA decreased the glass transition temperature (T_g) significantly from about 60 to 17 °C, whereas the melting temperature (T_m) did not drop significantly. Metallic nanoparticles increased the T_g; however, Ag–Cu alloy exhibited a greater increase than ZnO nanocomposite films. Particle size of ZnO NP did not show significant difference in the T_g values of the films. The T_m value of the nanocomposite films was not influenced by the NP. The addition of plasticizer initiated the crystallization (cold and melt) of the PLA/PEG blend, which was substantially improved by the incorporation of NP in the composite films, in particular, 1 mass% loading. Non-isothermal crystallization was significantly affected by the cooling and heating rates. Thermogravimetric analysis data indicated that only Ag–Cu alloy could improve the thermal stability of nanocomposite films. Furthermore, nanoparticles significantly influenced the UV barrier and the transmittance of plasticized films.

✉ Jasim Ahmed
jahmed2k@yahoo.com; jaahmed@kisr.edu.kw

[1] Food and Nutrition Program, Environment and Life Sciences Research Center, Kuwait Institute for Scientific Research, P.O. Box 24885, 13109 Safat, Kuwait

[2] School of Packaging, Michigan State University, East Lansing, MI 48824, USA

Keywords Poly(lactic acid) · Ag–Cu alloy nanoparticles · ZnO nanoparticles · Glass transition · Non-isothermal crystallization · Nanocomposite films

Introduction

Poly(lactic acid) (PLA) is a renewable, biodegradable and biocompatible thermoplastic material. PLA-based materials have received tremendous attention due to their versatile applications in drug delivery, tissue engineering, food packaging, household goods and automobile industry [1–4]. The production and development of biodegradable food packaging materials from PLA offers an advantage over traditional petrochemical-based plastic materials such as polystyrene, polyethylene and polypropylene providing an alternative disposal route (composting) and reducing the dependence of petroleum. The ease in processability and high transparency of PLA films compete with those of many conventional petrochemical plastics. Moreover, PLA has been approved as generally recognized as safe (GRAS) by the United States Food and Drug Administration (FDA), and it is safe for packaging of food materials [5, 6]. However, the applicability of PLA in packaging films has been restricted due to its relatively high resin cost, brittleness, poor toughness, inferior barrier properties, low thermal stability and slow crystallization rate [7, 8]. The thermal behavior of a polymer can be examined using differential scanning calorimetry (DSC) studies by detecting multiphase transitions such as glass transition, cold crystallization and melting. Among thermal properties, crystallization is one of the most important characteristics since mechanical properties and biodegradability of PLA significantly depend on its crystallinity [7, 9]. The most feasible method to improve thermal properties and overall crystallization rate of PLA is

the blending of polymer matrix and the introduction of nucleating agent into the polymer matrix [9].

To overcome the existing limitations and improve the mechanical performance of PLA, mostly plasticizers and fillers have been incorporated into PLA matrix [10]. Recently, nanotechnology has been introduced to modify the physical, mechanical and thermal properties of biopolymers to compete with the low-cost petro-chemical packaging materials. The incorporation of nanoparticles as particulate fillers into polymer matrices is a prominent technique to enhance or modify properties of neat polymers [11, 12]. Polymer nanocomposites are made by dispersing inorganic or organic nanoparticles into either a thermoplastic or thermoset polymer. Such nanoparticles offer enormous advantages over microparticles due to their large specific surface area and aspect ratio, excellent interfacial interactions on polymer branches, thus significantly enhancing polymer properties such as thermal, mechanical and water barrier properties [13]. Improved thermal, rheological, mechanical and barrier properties of nanocomposite polymers have been reported [14, 15].

Nanocomposites based on PLA have been reported by several research groups [11, 15, 16]. Recently, the incorporation of ZnO nanoparticles as functional filler into the PLA-based films has been reported to improve mechanical and water vapor barrier properties [17, 18]. However, the influence of two different particle fractions of ZnO nanoparticles (<50 and <100 nm) on properties of PLA film has rarely been studied. Moreover, the incorporation of novel bimetallic nanoparticles like Ag–Cu alloy as nanoscale fillers into the PLA matrix and thermal properties of resulting PLA/Ag–Cu alloy nanocomposites had never been reported before. Both ZnO and Ag–Cu alloy nanoparticles have shown excellent antimicrobial activity against food-borne pathogens and spoilage bacteria [19]. Therefore, the main objective of the present study was the preparation and exploration of thermal properties (i.e., glass transition, melting and crystallization) of PLA nanocomposite films using calorimetric technique as influenced by the incorporation of ZnO (<50 and <100 nm) and Ag–Cu alloy nanoparticles. In addition, the effect of heating and cooling rates on melt crystallization and cold crystallization behavior during non-isothermal conditions of nanocomposite has also been investigated. This information would be useful to better understand PLA/PEG/ZnO or PLA/PEG/Ag–Cu alloy nanocomposites and their melt processing, film development and possible applications.

Materials and methods

Chemicals

A commercial grade poly (lactic acid) (PLA) (Ingeo^{TM} 4043D)—average molecular mass (M_w) of 175 g mol^{-1} and number average molecular mass of 95 g mol^{-1}—was procured from Nature Works LLC (Minnetonka, MN, USA). Dichloromethane (DCM) was obtained from Fisher Scientific (Loughborough, LE, UK) and used as received. Poly ethylene glycol (PEG) (M_w = 1500 g mol^{-1}), zinc oxide (ZnO) nanoparticles (<50 and <100 nm) and silver–copper alloy (Ag–Cu) nanoparticles <100 nm were purchased from Sigma-Aldrich (St. Louis, MO, USA).

Composite film preparation

All PLA-based films [PLA, PLA/PEG, PLA/PEG/ZnO (<50 and <100 nm) and PLA/PEG/Ag–Cu alloy] were prepared by a solvent casting method. The detailed composition of the films is presented in Table 1. Before film preparation, PLA was dried overnight at 60 °C under vacuum. All ingredients were accurately weighed (2.000 ± 0.001 g), well mixed and dissolved in 60 mL of dichloromethane (DCM). The mixture was sonicated (Branson Ultrasonics, CT, USA) for 30 min to disperse the nanoparticles. The resultant solution was then poured onto a glass petri dish (10 cm diameter and 1.5 cm depth) and dried at room temperature for overnight under a fume hood to form the film. Films were peeled from the petri dishes and stored in a desiccator for another 24 h before the experiment.

Table 1 Details of PLA-based composite materials

Compositions	Composition
(A) Neat PLA	
PLA	100/0
(B) PLA/PEG blends	
PLA/PEG	95/5
PLA/PEG	90/10
PLA/PEG	85/15
PLA/PEG	80/20
(C) PLA/PEG/ZnO (<50 nm) composite films	
PLA/PEG/ZnO	79.5/20/0.5
PLA/PEG/ZnO	79/20/1
PLA/PEG/ZnO	78/20/2
PLA/PEG/ZnO	76/20/4
(D) PLA/PEG/ZnO (<100 nm) composite films	
PLA/PEG/ZnO	79.5/20/0.5
PLA/PEG/ZnO	79/20/1
PLA/PEG/ZnO	78/20/2
PLA/PEG/ZnO	76/20/4
(E) PLA/PEG/Ag–Cu alloy (<100 nm) composite films	
PLA/PEG/Ag–Cu alloy	79.5/20/0.5
PLA/PEG/Ag–Cu alloy	79/20/1
PLA/PEG/Ag–Cu alloy	78/20/2
PLA/PEG/Ag–Cu alloy	76/20/4

Film thickness

The thickness of the film was measured using a digital micrometer (Mitutoyo, Model ID-C112PM, Serial No. 00320, Mituyoto Corp., Kawasaki-shi, Japan). Ten random locations around each film sample were used for thickness determination.

Thermal properties measurement

Thermal analysis was carried out with a differential scanning calorimeter (DSC) (TA Q 2000, TA Instruments, New Castle, DE, USA), which was calibrated against an indium standard. An empty aluminum pan served as reference. The film specimens (10–12 mg) were heated and cooled in 2 heating–cooling cycles under nitrogen atmosphere (flow rate 50 mL min^{-1}) at a rate of 10 °C min^{-1}. In the 1st cycle, PLA samples were equilibrated at 180 °C and isothermed for 5 min; cooled to −80 °C at 10 °C min^{-1} and isothermed for 5 min; heated to 180 °C at 10 °C min^{-1} and isothermed for 3 min. Similar steps were followed in the 2nd cycle. The melting temperature (T_m) was taken at the end of the melting peak, whereas crystallization temperature (T_c) was considered as the minimum of the exothermic peak. The T_c observed during heating and cooling cycles were considered as cold (T_{cc}) and melt crystallization temperature (T_{mc}), respectively. The T_m was determined from the 1st heating cycle while crystallization and glass transition temperature (T_g) were calculated by the 2nd heating–cooling cycle. The crystallinity level (% $X_{cc,mc}$) was calculated based on the enthalpy of crystallization and/or melting, assuming the enthalpy of fusion of 93 J g^{-1} [20]. The non-isothermal crystallization studies were carried out in the cooling rate ranged from 2.5 to 20 °C min^{-1}. Thermal scans for each sample were carried out in triplicate, and the average values are reported. The area under the curve was calculated as the enthalpy from the instrument software.

Thermogravimetric analysis (TG)

The thermal stability of the films ($\approx$10 mg) was determined using a TG analyzer (TA Q 500, TA Instruments, New Castle, DE, USA) from 40 to 600 °C at a heating rate of 10 °C min^{-1} under nitrogen atmosphere. The mass loss of samples was recorded and plotted as a function of temperature.

UV-barrier and transparency of nanocomposite films

The UV-barrier and transparency of films was tested by measuring percent transmittance at 280 nm (T_{280}) and 660 nm (T_{660}), respectively, using a UV–visible spectrophotometer (Shimadzu UV-1800, Kyoto, Japan) according to the method described by Shankar et al. [21].

Results and discussion

Film thickness

The thickness of the PLA/PEG (80/20) film was 0.52 ± 0.01 mm, which increased to 0.63 ± 0.02, 0.69 ± 0.01 and 0.71 ± 0.03 mm after the incorporation of ZnO (50 nm), ZnO (100 nm) and Ag–Cu alloy (100 nm), respectively. The increase in the thickness is believed to be associated with the nanoparticles that possibly adhered to the film surface. A similar increase in film thickness has been reported by various researchers for nanocomposite films [14, 22].

Thermal analysis

Thermal analysis was carried out on neat, plasticized PLA, and nanocomposite PLA films, in order to investigate the influence of the plasticizer and fillers on the thermal properties of the produced films. Thermal analysis parameters such as glass transition temperature (T_g), melting temperature (T_m), melting enthalpy (H_m), crystallization temperatures (cold and melt) (T_c), crystallization enthalpy (H_c) and degree of crystallinity (% X_c) pertaining to PLA, plasticized PLA and nanocomposite films are summarized in Table 2.

Effect of PEG on plasticized PLA films

For the neat PLA, the T_g was about 60 °C (Fig. 1, Table 2), and the value dropped to around 50 and 17 °C when 5 and 20 mass% of PEG were incorporated in the blend (Fig. 2, Table 2). The T_g value in the PLA/PEG blend decreased with the increase in plasticizer content, and followed a linear relationship (Eq. 1). The decrease in T_g of PLA/PEG blend, has been attributed by enhanced segmental mobility of PLA chains caused by the presence of PEG, increasing with the PEG content. A similar drop in thermal properties of PLA/plasticizer blend has been reported [11, 23, 24].

$$T_{gPLA/PEG} = -2.11PEG + 60.67; \quad (R^2 = 0.99) \qquad (1)$$

Above the T_g, only traces of melting, at 134 °C, were detected on the curve of neat PLA; the enthalpy of the transition was equal to 9 J g^{-1}. The melting temperature for the PLA in the blends was not significantly different than the neat PLA. The T_m of the neat PLA dropped to 147.5 °C with addition of 20 mass% PEG (Table 2), indicating that plasticization did not affect the T_m of the

blend significantly. A similar observation was reported by Sungsanit, Kao and Bhattacharya [25], where authors observed a drop of 3–4 °C for PLA/PEG blend. The incorporation of PEG imparted the crystallinity in PLA/PEG blends. The neat PLA did not show any crystallinity during heating/cooling cycle; however, an introduction of 5 % PEG imparted the melt crystallization in the blend. With the increase in PEG content in the blend, the melt crystallization temperature (T_{cm}) dropped from 111 to 69 °C when the PEG content increased from 5 to 20 %, and the crystallization enthalpy ranged between 13 and 23 J g^{-1}. Furthermore, cold crystallization appeared in the blend when the PLA/PEG ratio maintained at 85/15 or more. The cold crystallization temperature (T_{cc}) dropped from 78 to 75 °C with addition of 20 % PEG in the blend, and the crystallization enthalpy increased, at best to 3–4 J g^{-1}. The plasticizers increased the ability of PLA to crystallize, which was demonstrated by a decrease in T_{cc} and an increase in the crystallization enthalpy. The increase in the crystallinity has been reported by various researchers for PLA plasticized with PEG and Polypropylene glycol (PPG) [11, 23, 26, 27].

Effect of nanoparticles on PLA nanocomposite films

The effect of nanoparticles incorporation into the plasticized PLA matrix on the T_g has been reported in Fig. 2, Table 2. The T_g values of PLA/PEG blend films increased by the incorporation of ZnO nanoparticles even at a loading of 0.5 %; however, no systematic increasing trend of T_g was found with the loading of nanoparticles (Fig. 2, Table 2). Effect of particle size on the T_g of the ZnO-based nanocomposite films indicated a difference. The T_g of 50-nm particles is higher at lower loading of ZnO (0.5–1 %); however, a reverse trend was observed at higher loading (2–4 %) where the T_g of 100-nm particles were higher compared to 50-nm particles. This increment of T_g may be influenced by the confinement of the polymer chains adjacent to the ZnO nanoparticles that prevent the segmental mobility of the polymer chains. The most significant improvement in the T_g was recorded in the PLA-based nanocomposite films when the Ag–Cu alloy nanoparticles were incorporated at a loading concentration of 1 mass% or above (Fig. 2, Table 2). The T_g of PLA/PEG (80:20) with 1 mass% Ag–Cu 1 mass% double compared with PLA/PEG 0.5 mass% Ag–Cu and then leveled off at higher loading concentration (2–4 %) (T_g = 35–36.4 °C) (Table 2). This result could be associated with loss of flexibility of the polymeric chains when the metallic nanoparticles could retard the chain mobility. Cacciotti et al. [28] observed an increment of T_g by 3 °C when 1 % Ag was loaded in PLA matrix. Noori and Ali [29] also reported that the incorporation of titanium oxide

Table 2 Effect of ZnO (<50 nm and <100 nm) and bimetallic Ag–Cu alloy (<100 nm) on thermal properties of PLA-based films

Sample	T_g/°C	T_m/°C	H_m/J g^{-1}	T_{cc}/°C	H_{cc}/J g^{-1}	T_{mc}/°C	H_{mc}/J g^{-1}	X_{cc}/%, X_{mc}/%
Neat PLA	60.3 ± 0.32	149.1 ± 0.1	9.4 ± 0.3	–	–	–	–	–
PLA:PEG (95:5)	49.8 ± 0.15	147.6 ± 0.06	23.5 ± 0.3	111.1 ± 0.2	22.9 ± 0.14	–	–	0.6 ± 0.04, –
PLA:PEG (90:10)	39.8 ± 0.12	147.2 ± 0.19	25.3 ± 0.06	99.6 ± 0.46	22.5 ± 0.15	–	–	3.0 ± 0.14, –
PLA:PEG (85:15)	30.8 ± 0.45	147.2 ± 0.2	20.7 ± 0.15	89.5 ± 0.31	18.2 ± 0.08	77.8 ± 0.03	2.9 ± 0.21	2.7 ± 0.08, 19.2 ± 1.1
PLA:PEG (80:20)	16.8 ± 0.33	147.5 ± 0.21	22.0 ± 0.22	69.2 ± 0.67	13.0 ± 0.42	75.2 ± 0.32	3.9 ± 0.12	9.6 ± 0.54, 19.5 ± 0.48
PLA (79.5 %) + PEG (20 %) + 0.5 % ZnO (<50 nm)	18.2 ± 0.11	150.0 ± 0.07	30.1 ± 0.24	78.7 ± 0.24	14.7 ± 0.26	79.7 ± 0.45	11.6 ± 0.04	16.5 ± 0.28, 19.9 ± 0.34
PLA (79 %) + PEG (20 %) + 1 % ZnO (<50 nm)	19.8 ± 0.57	150.2 ± 0.1	28.3 ± 0.15	83.4 ± 1.06	14.3 ± 0.4	78.6 ± 0.7	8.4 ± 0.22	15.1 ± 0.05, 21.4 ± 0.22
PLA (78 %) + PEG (20 %) + 2 % ZnO (<50 nm)	17.5 ± 0.28	149.3 ± 0.3	29.2 ± 0.17	77.8 ± 0.44	15.3 ± 0.14	77.1 ± 0.07	8.7 ± 0.23	14.9 ± 0.1, 22.1 ± 0.36
PLA (76 %) + PEG (20 %) + 4 % ZnO (<50 nm)	17.4 ± 0.23	149.9 ± 0.04	30.2 ± 0.23	79.5 ± 0.33	14.8 ± 0.24	79.9 ± 0.75	13.3 ± 0.24	16.6 ± 0.88, 18.1 ± 0.74
PLA (79.5 %) + PEG (20 %) + 0.5 % ZnO (<100 nm)	16.7 ± 0.09	150.1 ± 0.42	28.0 ± 0.15	83.4 ± 0.4	24.2 ± 0.4	75.5 ± 0.16	7.9 ± 0.23	4.1 ± 0.32, 21.6 ± 0.61
PLA (79 %) + PEG (20 %) + 1 % ZnO (<100 nm)	19.6 ± 0.1	150.7 ± 0.18	29.7 ± 0.06	85.1 ± 0.09	13.4 ± 0.52	78.7 ± 0.7	11.8 ± 0.09	17.5 ± 0.81, 19.3 ± 0.14
PLA (78 %) + PEG (20 %) + 2 % ZnO (<100 nm)	19.1 ± 0.26	150.1 ± 0.11	25.8 ± 0.37	84.9 ± 0.35	14.2 ± 0.25	76.9 ± 0.29	9.6 ± 0.09	12.5 ± 1.21, 17.4 ± 0.96
PLA (76 %) + PEG (20 %) + 4 % ZnO (<100 nm)	18.9 ± 0.17	149.6 ± 0.06	28.9 ± 0.2	82.3 ± 0.42	9.3 ± 0.42	80.3 ± 0.23	7.7 ± 0.11	21.1 ± 0.62, 22.8 ± 0.31
PLA (79.5 %) + PEG (20 %) + 0.5 % Ag–Cu alloy (<100 nm)	17.7 ± 0.24	149.2 ± 1.17	26.1 ± 0.19	84.3 ± 0.74	21.8 ± 0.61	75.1 ± 0.16	7.1 ± 0.16	4.6 ± 0.11, 20.4 ± 0.84
PLA (79 %) + PEG (20 %) + 1 % Ag–Cu alloy (<100 nm)	36.4 ± 0.26	149.1 ± 0.15	24.6 ± 0.11	82.4 ± 0.24	16.4 ± 0.05	77.2 ± 0.29	5.7 ± 0.21	8.8 ± 0.18, 20.4 ± 0.94
PLA (78 %) + PEG (20 %) + 2 % Ag–Cu alloy (<100 nm)	35.5 ± 0.31	148.8 ± 0.66	24.2 ± 0.09	79.6 ± 0.17	9.3 ± 0.08	75.9 ± 0.41	8.7 ± 0.1	16.0 ± 0.21, 16.6 ± 0.42
PLA (76 %) + PEG (20 %) + 4 % Ag–Cu alloy (<100 nm)	34.9 ± 0.37	148.7 ± 0.05	24.8 ± 0.14	82.2 ± 0.23	15.7 ± 0.21	76.3 ± 0.23	9.9 ± 0.2	9.8 ± 0.32, 16.1 ± 0.33

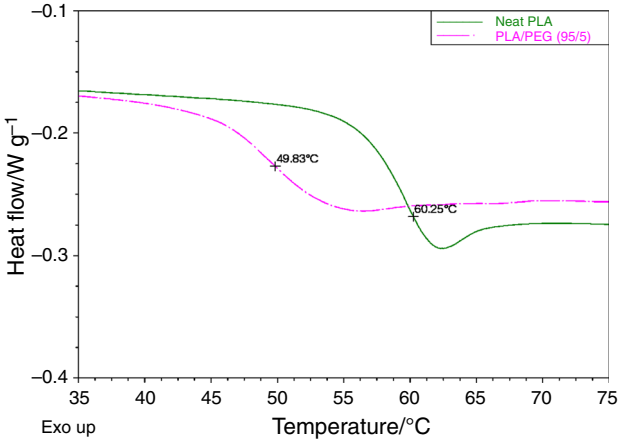

Fig. 1 Effect of 5 % PEG on glass transition of PLA film

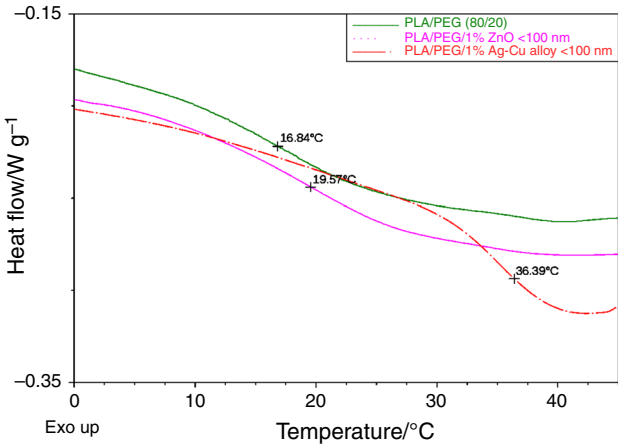

Fig. 2 Effect of ZnO (<50 nm) and Ag–Cu alloy (<100 nm) nanoparticles on glass transition of plasticized PLA/PEG (80/20) film

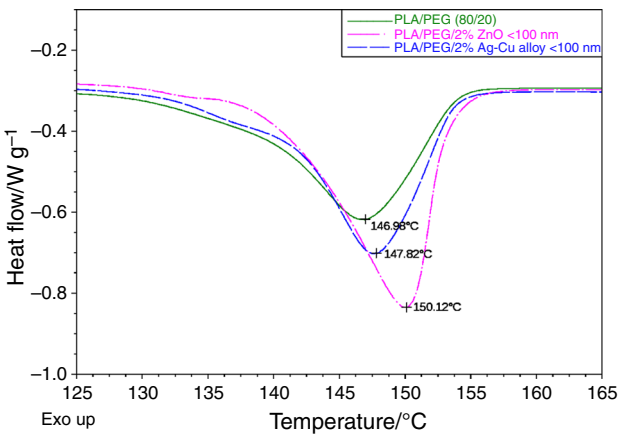

Fig. 3 Effect of ZnO (<100 nm) and Ag–Cu alloy (<100 nm) nanoparticles on melting temperature of plasticized PLA/PEG (80/20) film

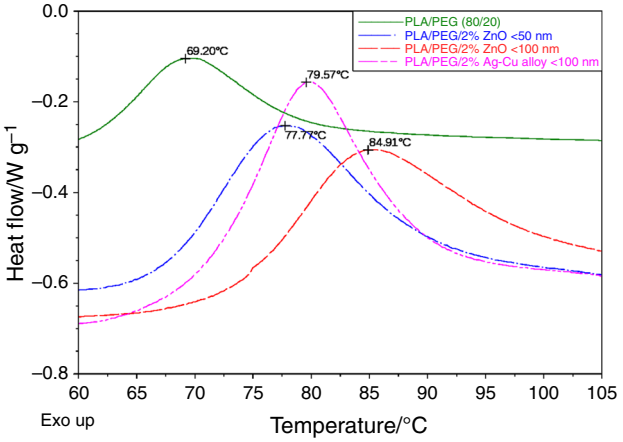

Fig. 4 Effect of ZnO (<50 and <100 nm) and Ag–Cu alloy (<100 nm) nanoparticles on cold crystallization of plasticized PLA film

and silver nanoparticles increases T_g of plasticized PLA film. The addition of nanoparticles to the PLA/PEG blend did not improve the T_m values significantly (Table 2; Fig. 3). It clearly indicated that the addition of ZnO or Ag–Cu alloy nanoparticles did not have a major influence on the T_m values of the nanocomposites, as compared to neat PLA. Similar observations on melting temperatures have been reported for Ag and graphene-loaded PLA nanocomposites [28, 30]. However, the process enthalpy varied between two nanoparticle-enriched films.

The addition of nanoparticles into PLA/PEG blend initiated the crystallization. The incorporation of ZnO and Ag–Cu alloy nanoparticles into plasticized PLA improved the crystallinity. The crystallization peaks attributed by PLA/PEG/2 % ZnO (<50 and <100 nm) and Ag–cu alloy nanocomposite films are illustrated in Fig. 4 and Table 2. The crystallization temperature of the plasticized nanocomposites increased regardless of nanoparticles and ranged between 74 and 80 °C; however, ZnO acted as a better nucleating agent than Ag–Cu alloy one. Besides, 100-nm particle size of ZnO exhibited higher crystallization temperature than 50-nm particle size at similar metal powder loading. ZnO 100-nm particles acted as a better nucleating agent in the nanocomposite films than 50-nm particles. The crystallization enthalpy varied significantly among films. A higher crystallization temperature suggests lower crystallization barrier energy, which can be attributed to the fact that NP can serve as crystallization nucleating agents, and thus effectively promote heterogeneous nucleation [31]. Cold crystallization phenomena induced via nanoparticle incorporation were also reported by other researchers [32, 33]. The degree of crystallinity of all nanocomposite films was almost alike.

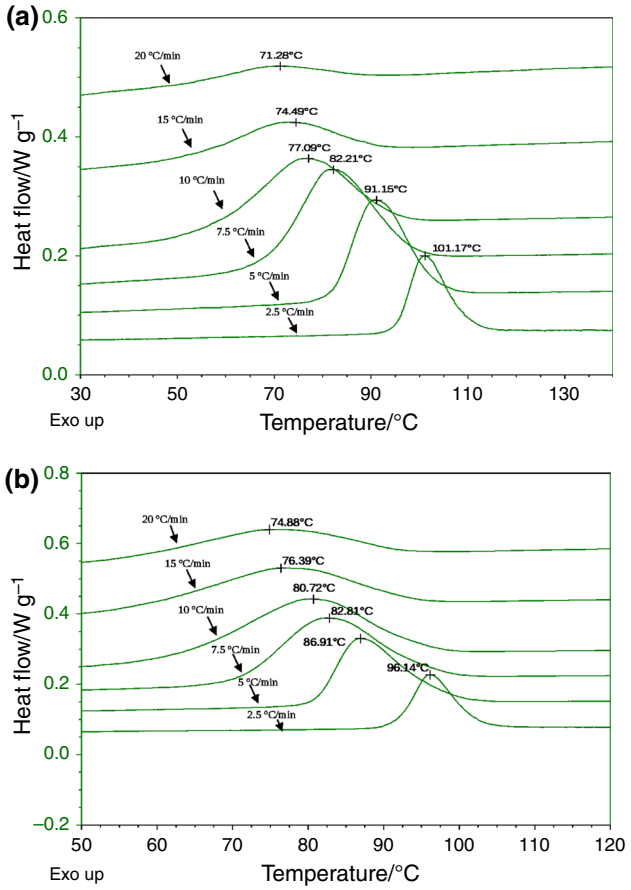

Fig. 5 Effect of cooling rate on the crystallization of PLA/PEG/2 % ZnO-100nm (**a**) and PLA/PEG/2 % Ag–Cu alloy (**b**) nanocomposite films

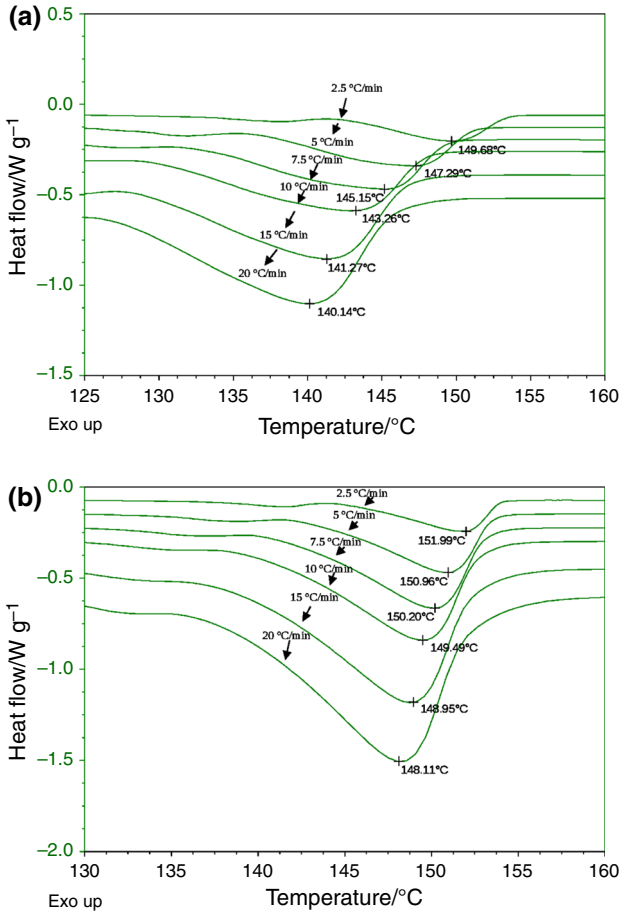

Fig. 6 Effect of cooling rate on melting of PLA/PEG/2 % ZnO (**a**) and PLA/PEG/2 % Ag–Cu alloy (**b**) nanocomposite films

Non-isothermal crystallization of PLA nanocomposites

The study of the crystallization and melting behavior of polymers and their nanocomposites is of great interest as it influences not only the crystalline structure and morphology but also the macroscopic characteristics of the materials [34]. The non-isothermal cold crystallization as a function of cooling rate of PLA/PEG/ZnO and PLA/PEG/Ag–Cu alloy nanocomposite film at 2 mass% loading is illustrated in Fig. 5. As the cooling rate increased from 2.5 to 20 °C min^{-1}, the crystallization temperature (T_c) decreased significantly. The crystallization temperature peak of both nanocomposite films shifted toward a lower value and became much wider with the increase in cooling rate. Similar trends have been reported by Ahmed et al. [35] for PLA. This phenomenon is common for crystallization of polymeric materials and can be ascribed to the kinetic effect in a nucleation-controlled region [36]. At a lower cooling rate, there is sufficient time for the molecules to arrange and the nuclei with a larger size to form, so that it stabilizes at a higher temperature. At a fast cooling rate (similar than quenching), the polymer molecules experienced a rapid decrease in temperature and the small produced nuclei do not time to growth and form crystals, so that the T_{cc} is found at a considerably lower temperature [35]. The crystallization peak temperature (T_c) was also influenced by nanoparticles and its nucleation capability. At a constant cooling rate of at 5 °C min^{-1}, the T_c of ZnO and Ag–Cu alloy-filled PLA nanocomposite films were 91.1 and 86.9 °C, respectively. It clearly indicates that Ag–Cu alloy had superior nucleation capability over ZnO. Furthermore, it has been reported that there is a competitive relevance between the crystallization rate and cooling rate during non-isothermal crystallization [37].

The melting behavior of 2 % metallic nanofiller incorporated composite (PLA/PEG/ZnO and PLA/PEG/Ag–Cu alloy) films at selected heating rates (2.5–20 °C min^{-1}) are illustrated in Fig. 6. The sharpness of melting peak increased with the increase in heating rate. At a slower heating rate (2.5 °C min^{-1}), the melting temperature T_m of PLA/PEG/ZnO film was detected at about 150 °C and the

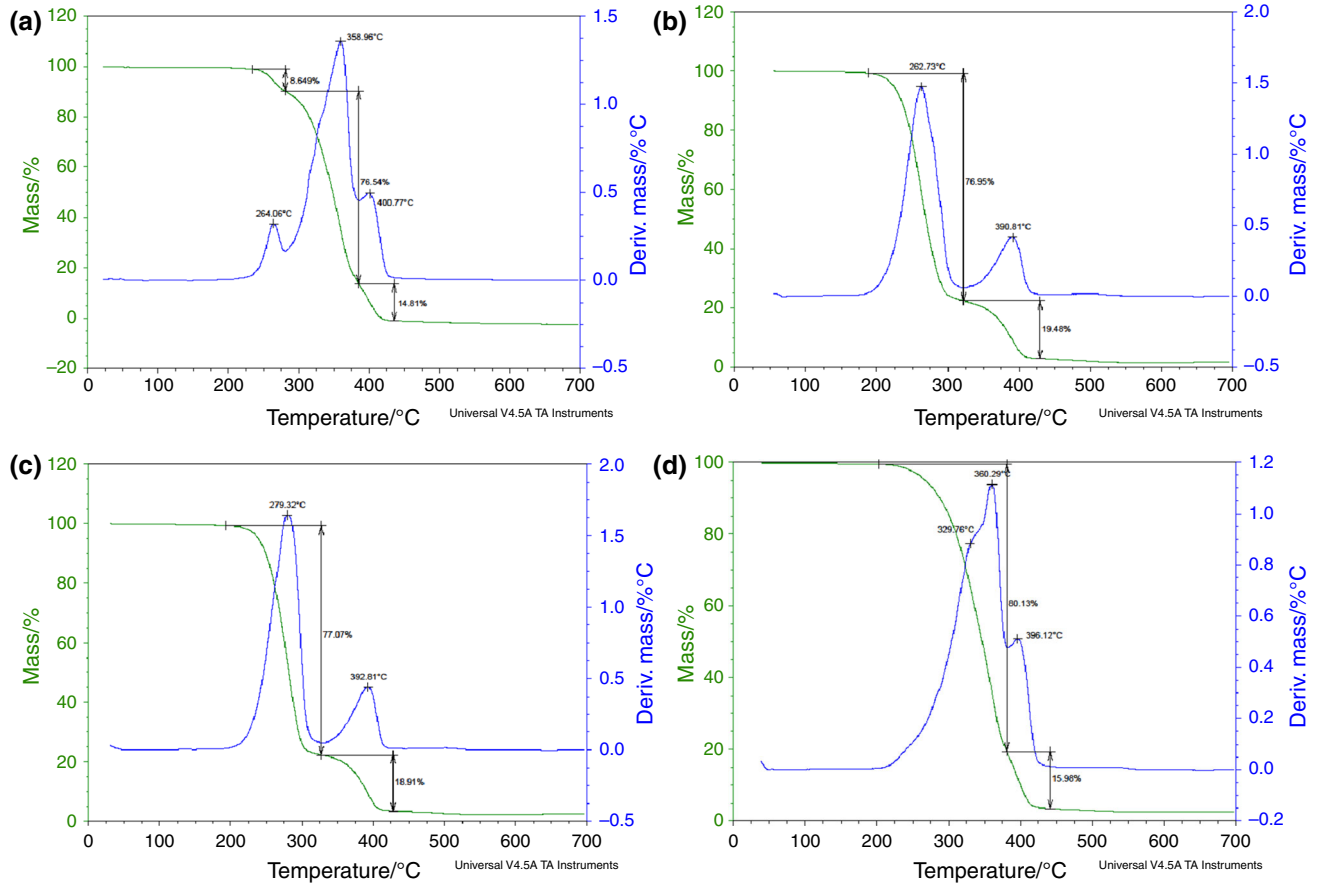

Fig. 7 TG of PLA/PEG (**a**), PLA/PEG/2 % ZnO < 50nm (**b**), PLA/PEG/2 % ZnO <100 nm (**c**) and PLA/PEG/2 % Ag–Cu alloy <100 nm composite films (**d**)

corresponding T_m value was about 140 °C at the fastest heating rate (20 °C min^{-1}). Similarly, the T_m values for PLA/PEG/Ag–Cu alloy were about 152 and 148 °C for the slowest and the fastest heating rate of 2.5 and 20 °C min^{-1}, respectively. The possible reason was that a faster heating rate exhibited a greater thermal inertia compared with the nucleating effect of nanoparticles. Samples heating at lower heating rate have more time to develop better crystals, so that the T_m shows higher values.

Thermogravimetric analysis

Molecular interaction or the bond dissociation of different macromolecules and inherent characteristics of the components are the major parameters involved in thermal stability of the polymeric nanocomposites. It has been established that the incorporation of nanoparticles is generally complemented with the improvement of the thermal properties of the matrix polymers [32]. In this work, the thermal stability and degradation profiles of plasticized PLA (PLA/PEG) and PLA/PEG/NP were measured by TG analyzer, and the results are illustrated in Fig. 7. Figure 7 shows that the PLA/PEG exhibited three-step degradation, whereas ZnO nanocomposite films exhibited two-step degradation only. Furthermore, it can be seen that all the test specimens were thermally stable below 260 °C, which is the normal processing temperature of PLA. The composites were able to maintain more than 95 % of their original mass at this temperature. A minor mass loss was recorded for the PLA/PEG film at temperature below 260 °C, which is believed to be associated with flash point of PEG (Fig. 7a). However, no mass loss was observed for nanocomposite films below 260 °C.

The PLA/PEG samples exhibited a major degradation at decomposition temperature of about 359 °C. However, PLA/PEG/ZnO nanocomposite films at 2 % ZnO loading showed major degradations at 262 and 272 °C, respectively, for 50- and 100-nm particle sizes. An improved thermal stability was expected for a nanocomposite prepared by incorporating thermally stable inorganic nanoparticles into the polymer matrix [38, 39]. However, nanoparticles act also as deformation accelerators at higher temperatures [40]. The lower peak decomposition temperatures of PLA/PEG/ZnO may indicate low thermal

stability at higher temperatures compared to PLA/PEG blend due to some M_w reduction during processing. A similar observation was made by Chang et al. [41] for PLA/MMT and Cloisite 25A nanocomposite films. However, the temperature value at the maximum decomposition rate, obtained from the derivative thermogravimetric (DTG) curves, of PLA/PEG/Ag–Cu alloy nanocomposite films was 458 °C, higher when compared to the temperature of control film (450 °C) or to the temperature of nanocomposite film with ZnO < 100 nm (438 °C). Thus, the nanocomposite film incorporated with bimetallic Ag–Cu alloy NP showed enhanced thermal stability in comparison with control film and ZnO nancomposite films. The resistance of Ag–Cu alloy nanocomposites toward thermal degradation may be related to the high thermal stability of bimetallic alloy nanoparticles and interaction between PLA matrix and Ag–cu alloy nanoparticles. The strong interaction between nanoparticles and the PLA matrix was also shown by the FTIR spectra and XRD patterns too (data not shown). Similar to our results, Mróz et al. [42] reported that the PLA composite with silver nanoparticles improves the thermal stability of PLA, as observed by an increase in decomposition temperature. The increase in the degradation temperature due to the incorporation of the nanoparticles into PLA can be explained by a shielding effect. The presence of additives disturbs the gas release from decomposed samples and delays a mass loss [42]. A comparison of the thermal stability results led to the conclusion that the PLA/PEG/ZnO thermally decomposed more easily than Ag–Cu alloy in the PLA matrix during heating.

The mass of the residue at 600 °C increased, for all nanocomposite films. However, PLA/PEG/Ag–Cu alloy films had higher residue content than others. The enhancement in char content observed in nanocomposite films is ascribed to the high heat resistance exerted by the nanoparticles itself [14]. From the TG data, it was clearly observed that Ag–Cu alloy nanoparticles were able to increase the char residue of the PLA/PEG films from 0.001 to 3.979 %.

UV-barrier and transparency of films

Transmission of UV and visible light at wavelength of 280 nm (T_{280}) and 660 nm (T_{660}) of neat PLA, PLA/PEG and PLA/PEG films incorporated with nanoparticles at different levels are shown in Table 3. The neat PLA film was transparent with high transmittance value at 660 nm (74.3 ± 0.7 %), whereas it had inferior UV barrier property as shown by high transmittance value at 280 nm (60.2 ± 2.2 %). Neat PLA-based films are generally known to have inferior UV barrier properties [43].

The percent transmittance (%T) of films in both UV and visible range decreased linearly as the PEG concentration increased from 5 to 20 %. With the incorporation of NPs to PLA/PEG (80/20) blend, the % T dropped significantly both at 280 and 660 nm. This result indicates that the NPs play an important role in blocking UV light through the films due to the absorbance of UV light by the nanoparticles dispersed in the film matrix (Table 3). ZnO-loaded PLA films had lower transmission in the UV range than Ag–Cu alloy PLA films. The nanocomposite films with strong UV barrier capacity could be used as UV-shielding packaging films to prevent UV light, which can induce lipid oxidation of various foods. Furthermore, the decrease in % T of nanocomposite films could be related to the opacity of NP, which was distributed throughout the films. Similar results have been reported by various researchers for nanocomposite films [14, 22, 44]. Thus, both PEG and NP impacted the transparency and light barrier properties of PLA based films.

Table 3 UV-barrier and transparency of PLA-based nanocomposite films

Film sample	T_{280nm}/%	T_{660nm}/%
PLA	60.2 ± 2.2	74.3 ± 0.7
PLA/PEG (95:5)	61.3 ± 2.1	72.5 ± 1.1
PLA/PEG (90:10)	59.2 ± 1.6	71.9 ± 0.4
PLA/PEG (85:15)	53.7 ± 1.4	70.3 ± 1.1
PLA/PEG (80:20)	49.2 ± 0.1	68.5 ± 1.0
PLA/PEG/0.5 % ZnO-50 nm	34.0 ± 1.1	56.9 ± 1.3
PLA/PEG/1 % ZnO-50 nm	24.1 ± 0.1	47.6 ± 0.1
PLA/PEG/2 % ZnO-50 nm	23.2 ± 0.1	43.0 ± 1.6
PLA/PEG/4 % ZnO-50 nm	3.8 ± 0.1	32.3 ± 1.9
PLA/PEG/0.5 % ZnO-100 nm	14.1 ± 1.0	41.2 ± 2.1
PLA/PEG/1 % ZnO-100 nm	8.7 ± 0.1	33.9 ± 3.5
PLA/PEG/2 % ZnO-100 nm	5.7 ± 1.2	28.5 ± 1.2
PLA/PEG/4 % ZnO-100 nm	2.1 ± 0.1	22.4 ± 0.7
PLA/PEG/0.5 % Ag–Cu alloy	27.5 ± 3.2	29.0 ± 1.3
PLA/PEG/1 % Ag–Cu alloy	20.4 ± 2.2	17.1 ± 0.1
PLA/PEG/2 % Ag–Cu alloy	15.8 ± 1.4	12.4 ± 0.1
PLA/PEG/4 % Ag–Cu alloy	7.2 ± 1.2	7.5 ± 1.2

Conclusions

Poly(lactic acid)-based bionanocomposites were prepared by incorporating metallic nanoparticles in solution. Thermal properties (glass transition, melting and crystallization) of the nanocomposites showed that the incorporation of nanoparticles especially Ag–Cu alloy into the PLA matrix led to the significant changes in the thermal behavior especially glass transition of the nanocomposite films. Both ZnO (<50 and <100 nm) and Ag–Cu alloy nanoparticles acted as nucleating agents and improved the crystallization

behavior of the films. The non-isothermal crystallization of nanocomposites was significantly influenced by the cooling/heating rates. TG analysis confirmed that only Ag–cu alloy nanoparticles could improve the thermal stability of PLA/PEG films. The nanocomposite films showed strong UV barrier capacity as compared to neat PLA. These biodegradable nanocomposites show great potential as an alternative to synthetic petrochemical-based packaging materials especially for use in food packaging and biodegradability.

Acknowledgements The authors express their gratitude to the Kuwait Institute for Scientific Research for providing the grant for the research work (Grant number FB087C).

References

1. Boccaccini AR, Notingher I, Maquet V, Jérôme R. Bioresorbable and bioactive composite materials based on polylactide foams filled with and coated by Bioglass® particles for tissue engineering applications. J Mater Sci Mater Med. 2003;14:443–50.
2. Ahmed J, Varshney SK. Polylactides—chemistry, properties and green packaging technology: a review. Int J Food Prop. 2011;14:37–58.
3. Bai H, Huang C, Xiu H, Zhang Q, Deng H, Wang K, Chen F, Fu Q. Significantly improving oxygen barrier properties of polylactide via constructing parallel-aligned shish-kebab-like crystals with well-interlocked boundaries. Biomacromolecules. 2014;15:1507–14.
4. Yu Y, Chen CK, Law WC, Weinheimer E, Sengupta S, Prasad PN, Cheng C. Polylactide-graft-doxorubicin nanoparticles with precisely controlled drug loading for pH-triggered drug delivery. Biomacromolecules. 2014;15:524–32.
5. Jamshidian M, Tehrany EA, Imran M, Jacquot M, Desobry S. Poly-lactic acid: production, applications, nanocomposites, and release studies. Compr Rev Food Sci Food Saf. 2010;9:552–71.
6. FDA. Inventory of effective food contact substance (FCS). 2002; Notifications No. 178. http://www.accessdata.fda.gov/scripts/fcn/fcnDetailNavigation.cfm?rpt=fcsListing&id=178.
7. Liang JZ, Zhou L, Tang CY, Tsui CP. Crystalline properties of poly(L-lactic acid) composites filled with nanometer calcium carbonate. Compos B Eng. 2013;45:1646–50.
8. Zhao H, Cui Z, Wang X, Turng LS, Peng X. Processing and characterization of solid and microcellular poly(lactic acid)/polyhydroxybutyrate-valerate (PLA/PHBV) blends and PLA/PHBV/clay nanocomposites. Compos B Eng. 2013;51:79–91.
9. Ebadi-Dehaghani H, Barikani M, Khonakdar HA, Jafari SH. Microstructure and non-isothermal crystallization behavior of PP/PLA/clay hybrid nanocomposites. J Therm Anal Calorim. 2015;121:1–12.
10. Auras R, Lim LT, Selke SE, Tsuj H. Poly (lactic acid): synthesis, structure, properties, processing and applications. Hoboken: Wiley; 2010.
11. Ahmed J, Varshney SK, Auras R. Rheological and thermal properties of polylactide/silicate nanocomposites films. J Food Sci. 2010;75:N17–24.
12. Swain SK, Isayev AI. Effect of ultrasound on HDPE/clay nanocomposites: rheology, structure and properties. Polymer. 2007;48:281–9.
13. Kovacevic V, Vrsaljko D, Blagojevic SL, Leskovac M. Adhesion parameters at the interface in nanoparticulate filled polymer systems. Polym Eng Sci. 2008;48:1994–2002.
14. Arfat YA, Benjakul S, Prodpran T, Sumpavapol P, Songtipya P. Properties and antimicrobial activity of fish protein isolate/fish skin gelatin film containing basil leaf essential oil and zinc oxide nanoparticles. Food Hydrocolloid. 2014;41:265–73.
15. Ray SS, Yamada K, Okamoto M, Fujimoto Y, Ogami A, Ueda K. New polylactide/layered silicate nanocomposites. 5. Designing of materials with desired properties. Polymer. 2003;44:6633–46.
16. Rhim JW, Hong SI, Ha CS. Tensile, water vapor barrier and antimicrobial properties of PLA/nanoclay composite films. LWT Food Sci Technol. 2009;42:612–7.
17. Jayaramudu J, Das K, Sonakshi M, Reddy GSM, Aderibigbe B, Sadiku R, Ray SS. Structure and properties of highly toughened biodegradable polylactide/ZnO biocomposite films. Int J Biol Macromol. 2014;64:428–34.
18. Pantani R, Gorrasi G, Vigliotta G, Murariu M, Dubois P. PLA-ZnO nanocomposite films: water vapor barrier properties and specific end-use characteristics. Eur Polym J. 2013;49:3471–82.
19. Espitia PJP, et al. Physical–mechanical and antimicrobial properties of nanocomposite films with pediocin and ZnO nanoparticles. Carbohydr Polym. 2013;94:199–208.
20. Fisher EW, Sterzel HJ, Wegner G. Investigation of the structure of solution growth crystals of lactide copolymers by means of chemical reactions. Kolloid-ZUZ Polym. 1973;251:980–90.
21. Shankar S, Teng X, Li G, Rhim JW. Preparation, characterization, and antimicrobial activity of gelatin/ZnO nanocomposite films. Food Hydrocolloid. 2015;45:264–71.
22. Kanmani P, Rhim JW. Physical, mechanical and antimicrobial properties of gelatin based active nanocomposite films containing AgNPs and nanoclay. Food Hydrocolloid. 2014;35:644–52.
23. Kulinski Z, Piorkowska E, Gadzinowska K, Stasiak M. Plasticization of poly (L-lactide) with poly (propylene glycol). Biomacromolecules. 2006;7:2128–35.
24. Chieng BW, Ibrahim NA, Wan-Yunus WMZ, Hussein MZ. Plasticized poly(lactic acid) with low molecular weight poly(-ethylene glycol): mechanical, thermal, and morphology properties. J Appl Polym Sci. 2013;130:4576–80.
25. Sungsanit K, Kao N, Bhattacharya SN. Properties of linear poly (lactic acid)/polyethylene glycol blends. Polym Eng Sci. 2012;52:108–16.
26. Martin O, Averous L. Poly (lactic acid): plasticization and properties of biodegradable multiphase systems. Polymer. 2001;42:6209–19.
27. Baiardo M, Frisoni G, Scandola M, Rimelen M, Lips D, Ruffieux K, Wintermantel E. Thermal and mechanical properties of plasticized poly (L-lactic acid). J Appl Polym Sci. 2003;90:1731–8.
28. Cacciotti I, Fortunati E, Puglia D, Kenny JM, Nanni F. Effect of silver nanoparticles and cellulose nanocrystals on electro-spun poly(lactic) acid mats: morphology, thermal properties and mechanical behavior. Carbohyd Polym. 2014;103:22–31.
29. Noori FTM, Ali NA. Study the mechanical and thermal properties of biodegradable polylacticacid/poly ethylene glycol nanocomposites. Int J App Innov Eng Manag. 2014;3:459–64.
30. Chieng BW, Ibrahim NA, Yunus WMZW, Hussein MZ. Poly (lactic acid)/poly (ethylene glycol) polymer nanocomposites: effects of graphene nanoplatelets. Polymer. 2013;6:93–104.
31. Mi HY, Li Z, Turng LS, Sun Y, Gong S. Silver nanowire/thermoplastic polyurethane elastomer nanocomposites: thermal, mechanical, and dielectric properties. Mater Design. 2014;56:398–404.
32. Lee SJ, Hahm WG, Kikutani T, Kim BC. Effects of clay and POSS nanoparticles on the quiescent and shear-induced crystallization behavior of high molecular weight poly(ethylene terephthalate). Polym Eng Sci. 2009;49:317–23.
33. Fortunati E, Armentano I, Zhou Q, Puglia D, Terenzi A, Berglund LA, Kenny JM. Microstructure and non-isothermal cold crystallization of PLA composites based on silver nanoparticles and nano-crystalline cellulose. Polym Deg Stab. 2012;97:2027–36.

34. Díez-Pascual AM, Díez-Vicente AL. Poly (3-hydroxybutyrate)/ZnO bionanocomposites with improved mechanical, barrier and antibacterial properties. Int J Mol Sci. 2014;15:10950–73.
35. Ahmed J, Zhang JX, Song Z, Varshney SK. Thermal properties of polylactides. J Therm Anal Calorim. 2009;95:957–64.
36. Supaphol P, Thanomkiat P, Junkasem J, Dangtungee R. Non-isothermal melt-crystallization and mechanical properties of titanium (IV) oxide nanoparticle-filled isotactic polypropylene. Polym Test. 2007;26:20–37.
37. Cai YH, Tang Y, Zhao LS. Poly (l-lactic acid) with the organic nucleating agent N, N, N′-tris (1H-benzotriazole) trimesinic acid acethydrazide: crystallization and melting behavior. J Appl Polym Sci. 2015;132:32.
38. Fischer HR, Gielgens LH, Koster TPM. Nanocomposites from polymers and layered minerals. Acta Polym. 1999;50:122–6.
39. Petrovic XS, Javni I, Waddong A, Banhegyi GJ. Structure and properties of polyurethane–silica nanocomposites. J Appl Polym Sci. 2000;76:133–51.
40. Ogata N, Jimenez G, Kawai H, Ogihara T. Structure and thermal/mechanical properties of poly (l-lactide)-clay blend. J Polym Sci Part B Polym Phys. 1997;35:389–96.
41. Chang JH, An YU, Sur GS. Poly(lactic acid) nanocomposites with various organoclays. I. Thermomechanical properties, morphology, and gas permeability. J Polym Sci Part B Polym Phys. 2003;41:94–103.
42. Mróz P, Białas S, Mucha M, Kaczmarek H. Thermogravimetric and DSC testing of poly(lactic acid)nanocomposites. Thermochim Acta. 2013;573:186–92.
43. Ligot S, Benali S, Ramy-Ratiarison R, Murariu M, Snyders R. Mechanical, optical and barrier properties of PLA-layered silicate nanocomposites coated with organic plasma polymer thin films. Mater Sci Eng Adv Res. 2015;2015(1):1.
44. Murariu M, Doumbia A, Bonnaud L, Dechief AL, et al. High-performance polylactide/ZnO nanocomposites designed for films and fibers with special end-use properties. Biomacromolecules. 2011;12:1762–71.